Nanoscale Research Letters

NANO EXPRESS Open Access

Facile Preparation of Carbon Nanotube-Cu_2O Nanocomposites as New Catalyst Materials for Reduction of P-Nitrophenol

Yao Feng[1,2], Tifeng Jiao[1,2*], Juanjuan Yin[2], Lun Zhang[2], Lexin Zhang[2*], Jingxin Zhou[2] and Qiuming Peng[1]

Abstract

The effective synthesis and self-assembly of nanocomposites were of key importance for a broad range of nanomaterial applications. In this work, new carbon nanotube (CNT)-Cu_2O nanocomposites were successfully synthesized via a facile approach. CNT was selected as the anchoring substrate to load Cu_2O nanoparticles to prepare composite catalysts with well stability and good reusability. It is discovered that the prepared CNT-Cu_2O nanocomposite materials could be effectively controlled via regulating preparation temperature and time without the use of any stabilizing agents. The nanostructures of synthesized composites were well characterized by many techniques, such as scanning electron microscopy (SEM), transmission electron microscopy (TEM), and X-ray diffraction (XRD). And the prepared CNT-Cu_2O nanocomposites with optimized preparation conditions as new catalyst displayed excellent catalytic performance on the reduction reaction of p-nitrophenol, demonstrating potential applications for environmental governance and composite materials.

Keywords: Nanocomposite, Cuprous oxide, Carbon nanotube, Catalytic reduction, P-nitrophenol

Background

Since the discovery of carbon nanotubes (CNT), the related research and applications for catalysts [1, 2], flexible supercapacitors [3], electronic sensors [4], and sustainable wastewater treatment [5] have been widely explored. It is well known that CNTs are special materials owing to high chemical stability, well electrical conductivity, large specific surface area, and extremely high mechanical strength [6]. These special properties make CNTs a great favor to researchers. In recent years, more research work on CNT catalysis have been conducted, most of which are related to composites with transition metals. For example, Karimi-Maleh et al. have synthesized CuO/CNTs nanocomposite by chemical precipitation method used as high adhesive carbon paste electrode [7, 8]. With the recent development of nanoscience and nanotechnology, developing a facile and low-cost strategy for synthesizing multi-functional carbon material is an important challenge. At the same time, more and more nanomaterials have been researched for improving catalytic properties, such as Pd [9], TiO [10], Mo [11], Zn [12], Au [13], and Ag [14]. Liu et al. used zinc to fabricate chloroplast mimics by the self-assembled approach, which was beneficial for photoenzymatic reaction in sustainable fuel synthesis [15]. Silver nanoparticles, for example, are now widely used as catalysts due to high reactivity and selectivity [16, 17]. In addition, Pt nanoparticles could serve as an electron separator [18]. Pt and TiO_2 acted as self-mineralization to reform the fiber bundles architecture [19]. Liu et al. researched the peptide-porphyrin co-assemblies; in this, they presented Pt nanoparticles easily mineralized [20]. A dendritic pyrenyl-moiety-decorated hyperbranched polyglycidol (pHBP) was prepared by Li and coworkers, which accomplished to functionalize CNTs via a non-covalent (non-destructive) process, after that Au, Ag, and Pt nanoparticles with uniform SiO_2, GeO_2, and TiO_2 coatings were deposited in situ onto the as-prepared CNT/pHBP hybrids [21]. Novel CNT/pHBP/Au hybrids and CNT/pHBP/Pt had been reported and showed excellent catalytic activity for 4-NP reduction

* Correspondence: tfjiao@ysu.edu.cn; zhanglexin@ysu.edu.cn
[1]State Key Laboratory of Metastable Materials Science and Technology, Yanshan University, Qinhuangdao 066004, People's Republic of China
[2]Hebei Key Laboratory of Applied Chemistry, School of Environmental and Chemical Engineering, Yanshan University, Qinhuangdao 066004, People's Republic of China

[13, 21]. In addition, the research group of Szekely achieved an excellent work about azido-derivatized cinchona-squaramide bifunctional catalyst grafted to the surface of polybenzimidazole-based nanofiltration membrane, which confirmed the change in geometry and increased secondary interactions, and enhanced the catalytic effect [22].

On the other hand, copper nanocrystals belonged to low-cost and higher abundance materials used as catalysts. The size and shape impacted on the catalytic activity, while the surface microstructures and arrangement of Cu atoms on the surface also determined the catalytic results [23]. Meldal [24] and Sharpless [25] had explored the ability of Cu^+ salts at room temperature or with moderate heating to speed up some cycloaddition reaction [26]. With functionalization of Cu catalysts, Cu nanomaterials were effectively used for electrocatalysis, photocatalysis, and CO_2 catalysis. For example, previous reports put forward that Cu was applied to the field of visible light active photocatalyst [27]. In that work, the simultaneous functionalization of Cu and Cd catalysts and photocatalytic CO_2 reduction were realized successfully. Copper nanostructures were also used in catalytic oxidation reactions, but these mechanisms are different from other metal catalysts [28]. Because CNTs demonstrated high mechanical strength, high thermal and electrical conductivity and adsorption, unique nanostructure, mechanical and thermal properties, and hydrophobicity, many researchers applied CNTs as templates to support for heterogeneous catalysts [29]. Hybrid nanoflower composites mixed with CNTs showed high enzyme wiring efficiency and electron transfer rate which could be used in the field of fabricating enzymatic biofuel cells [30]. In addition, Esumi's group explored the dendrimer-encapsulated Au NPs for 4-NP reduction, but the results showed the process influenced by the concentration and generation of the dendrimers [13, 31–33]. At the same time, some research work about CNT and Cu composites had been reported. Typically, Leggiero et al. found that the seeded Cu using the CVD method and electrodeposited with CNT achieved excellent conductors [34]. Cho et al. explored CNT and metal matrix composite-compounded chromium carbide by in situ formation, which achieved incompatible properties including electrical conductivity and temperature coefficient of resistance [35].

Herein, we report the synthesis of stable CNT-Cu_2O nanocomposites by a simple and easy way of preparation. Cu_2O nanocrystals were prepared from CuCl precursor. We adjusted different preparation temperatures and time to regulate the sizes of the formed Cu nanostructures. The method introduced in the previous report is relatively complexed, while the preparation approach in the present case seemed simple and eco-friendly with low material cost. Also, the as-prepared composite materials could be used as new catalytic materials and utilized for the reduction reaction of 4-NP [36]. Particularly, our study could display great potential applications in the wastewater treatment field and composite catalyst materials field.

Methods

The experiment used materials, multi-walled amination carbon nanotubes (95%, inner diameter of 3–5 nm, external diameter of 8–15 nm, length of 50 μm), cuprous chloride (97%, CuCl), and cupric chloride (98%, $CuCl_2$) were purchased from Aladdin Chemicals. Sodium hydroxide (96%, NaOH) was purchased from Tianjin Kermel Chemical Reagent. L-ascorbic acid (99.7%), sodium borohydride (98%, $NaBH_4$), and p-nitrophenol (98%, 4-NP) were purchased from Shanghai Hushi Reagent. All used solvents were of analytical grade and directly used without further treatment.

The targeted nanocomposites were synthesized by the following procedure: the mixture of 100 mg carboxylated carbon nanotubes and 100 mg CuCl solid was added into 250 mL deionized water in a clean beaker with magnetic string (300 r/min) for 20 min at 30 °C. Subsequently, keeping stirring for 1 h, 0.88 g ascorbic acid and 5.0 mL NaOH (1 M) were added into the above mixing solution. Then, the solid was washed with 100 mL ethanol and 100 mL deionized water for several times and was collected by drying in a vacuum at 50 °C for 48 h [16]. For comparison, different experimental conditions were controlled at 30 °C with stirring for 6 h or at 60 °C with stirring for 1 h. All the obtained samples were dried in a vacuum at 50 °C for 48 h.

The catalytic experiments were carried out and detected according to the previous reports [16]. In catalytic experiments, 0.0174 g 4-NP and 0.1892 g $NaBH_4$ were dissolved into 25 mL deionized water, respectively, and about 16 mL of 4-nitrophenol aqueous solution (0.313 mM) and a freshly prepared 15 mL sodium borohydride solution were added into a beaker at room temperature [36, 37]. Then, the synthesized CNT/Cu_2O composites (10 mg) were dispersed in the above-prepared solution to obtain a suspension. For standardizing instrument, 1.5 mL deionized water was added into a quartz cuvette and monitored using a UV-vis spectrophotometer at a wavelength from 220 to 550 nm. After that, every 4 min intervals, 1.5 mL supernatant liquid was monitored and recycled, which kept constant concentration in the reaction system. After the catalytic reaction, the used catalyst was recovered by centrifugation and washed with ethanol and water several times.

The morphologies of prepared composites were analyzed by employing a field-emission scanning electron microscope (SEM) (S-4800II, Hitachi, Japan) with the accelerating voltage of 15 kV. EDXS analysis was

typically performed at 200 kV acceleration using an Oxford Link-ISIS X-ray EDXS microanalysis system attached to SEM. Transmission electron microscopy (TEM, HT7700, Hitachi High-Technologies Corporation) was investigated with commercial 300-mesh copper grids. With an accelerating voltage of 200 kV, elemental mappings in composites were distinguished utilized to X-ray spectroscopy (EDXS). The composites were performed with a motorized sample stage of Horiba Jobin Yvon Xplora PLUS confocal Raman microscope equipped [38–42]. X-ray diffraction (XRD) analysis was investigated on an X-ray diffractometer equipped with a Cu Kα X-ray radiation source and a Bragg diffraction setup (SmartLab, Rigaku, Japan).

Results and Discussion

Firstly, Fig. 1 demonstrated the nanostructures of the synthesized CNT-Cu_2O nanocomposites via carbon nanotubes and cuprous chloride. After attempting the characterization of different parameters, the optimal products were obtained under different reaction factors. As shown in Fig. 1a, d, with reaction temperature 30 °C and stirring for 1 h, the size of Cu_2O nanocrystallines showed about 30–50 nm evenly distributed on the surface of nanotubes in the synthesized CNT-Cu-30-1 composite. In addition, the obtained composites under 30 °C and stirred for 6 h or 60 °C for 1 h, named as CNT-Cu-60-1 and CNT-Cu-30-6, have also been investigated, displaying big blocks of Cu_2O nanocrystalline particles even with the diameters at the micrometer scale. In order to further analyze the component dispersion of the prepared CNT-Cu-30-1 composite, we examined the morphologies by using EDS map scanning. Figure 2 showed the SEM image of CNT-Cu-30-1 nanocomposite and elemental mappings of C, O and Cu elements. The obtained results demonstrated the used carbon nanotubes could serve as a good carrier while the formed Cu_2O nanoparticles evenly adhered on the surface of CNT, which could be speculated to show good catalytic performances.

Next, the synthesized CNT-Cu_2O nanocomposites were characterized by XRD technique, as shown in Fig. 3. It is easily observed that the characteristic diffraction peak of CNT appeared at 2θ values of 26°, which could be indexed to PDF26–1079 owing to its carbon nanotube structure. In addition, many strong and sharp characteristic peaks could be assigned to Cu_2O nanocrystalline indexed to PDF05–0667. Apparently, all obtained composite samples showed the same characteristic peaks without any other impurities. It was interesting to note that for exploring the stability of Cu_2O nanoparticles, the obtained composite after 1 month was analyzed repeatedly by XRD. And the obtained result demonstrated the same curves, indicating the well stability of synthesized Cu_2O nanoparticles. In addition, the Raman spectra of CNT and the synthesized CNT-Cu_2O nanocomposites were investigated and shown in Fig. 4. Comparing CNT spectra with CNT-Cu-30-1 and CNT-Cu-60-1 spectra, all curves showed two distinct visible peaks (G and D) and a smaller one (2D), proving the existence of a carbon-based matrix. D peak (1344 cm^{-1}) represented the defects and disorders in CNT, and G peak (1605 cm^{-1}) indicated the result of disorder in sp^2-hybridized carbon systems. Moreover, 2D peak (2693 cm^{-1}) could be attributed to two-phonon lattice vibrations in CNT structure. It should be noted that in Fig. 4, the intensity ratio of the D and G peaks (I_D/I_G) for CNT showed the value of 1.64. However, the value of I_D/I_G of CNT-Cu-30-1 composite (1.34) suggested to be smaller than CNT but larger than CNT-Cu-60-1 composite (1.29). Owing to the higher the ratio, the bigger the defect of carbon crystal, which further demonstrated that the crystallinity of CNT-Cu-60-1 composite seemed larger than CNT-Cu-30-1, matching well with the results from the SEM characterization. On the other hand, characteristic peaks at 223 cm^{-1} and 485 cm^{-1} represented lattice vibrations in Cu_2O crystal.

The obtained CNT-Cu_2O nanocomposites have been utilized to reduce 4-nitrophenolate (4-NP) to 4-aminophenol (4-AP) solution in the presence of $NaBH_4$ as a typical reaction model. It was well reported that UV-vis spectroscopy was a distinct method to monitor 4-NP reduction reaction [23, 36, 38], which was widely studied. At first, the 4-NP solution with fresh aqueous $NaBH_4$ was monitored by UV-vis spectroscopy, as shown in Fig. 5. The maximum absorption peak of 4-NP was located at 314 nm. After the addition of $NaBH_4$ solution without the catalyst, the solution appeared bright yellow with peak position transferred to 401 nm, indicating the formation of 4-nitrophenolate [36]. As shown in Fig. 5a, the prepared CNT-Cu-30-1 composite could completely catalyze 4-NP mixtures with $NaBH_4$ to produce 4-aminophenol within 35 s, which could be mainly owing to the high catalytic capability of Cu_2O nanoparticles in this composite. In addition, when the catalysts of CNT-Cu-60-1 or CNT-Cu-30-6 were added into the reaction mixture, the maximum absorbance peak at 401 gradually disappeared after about 11–12 min, which suggested the formation of product 4-AP. At the same time, as presented in Fig. 5d, the color of the 4-NP solution with $NaBH_4$ changed from bright yellow to colorless state after the catalytic process, indicating the completion of the catalytic process.

It seemed an important indicator for catalyst materials to possess excellent stability and reutilization performances [43–52]. The continuous process made it sustainable and gained increasing attention, which seemed better than the batch process. Improving the circulation ability of composite helped to reduce the production cost. Thus, based on the above results of catalytic tests, we investigated the reusability of the synthesized

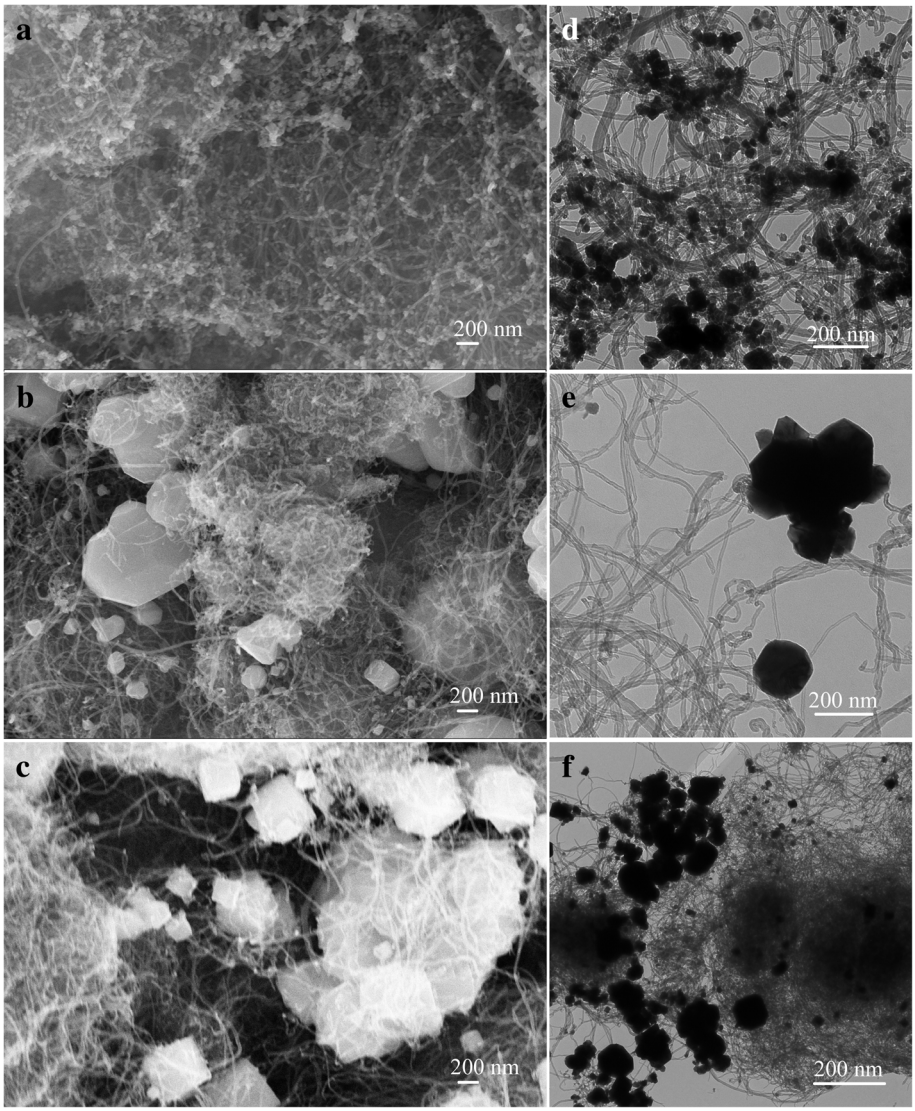

Fig. 1 SEM and TEM images of the synthesized CNT-Cu_2O nanocomposites. **a**, **d** CNT-Cu-30-1. **b**, **e** CNT-Cu-60-1. **c**, **f** CNT-Cu-30-6

CNT-Cu-30-1 nanocomposite as a catalyst for the reduction of 4-nitrophenol with $NaBH_4$ for subsequent eight times as a model. As shown in Fig. 6, the catalytic efficiency of the first round reached nearly 99% and showed the value of 92% even after 8 times, demonstrating excellent stability and reutilization of present synthesized nanocomposites. The possible reason of catalytic degradation could be attributed to the following: first, the active sites of composites were covered by trace residual 4-NP or 4-AP. Second, there was a trace loss when the catalyst was recycled and washed. To avoid these situations, magnetic nanoparticles could be added to future designs to reduce loss. Figure 7 displayed the preparation of CNT-Cu_2O nanocomposites and their catalytic properties on nitro-compounds. The scheme indicated that the preparation temperatures and time seemed to play an important role in regulating the sizes of Cu_2O nanocrystal and next catalytic performance. L-ascorbic acid was added into the reaction system as a reducing agent and Cu_2O were formed. And CNT acted as a substrate carrier to provide larger platform and anchoring sites to prevent agglomeration of Cu_2O nanoparticles. In addition, the combination of CNT with Cu_2O could enhance the process of electron transfer, which also increased intermolecular interactions between CNT and Cu_2O. In other reported studies, the reduction reaction of 4-NP was catalyzed by Cu nanowires with a time of 13 min [23]. Thus, present synthesized CNT-Cu_2O-1 achieved high catalytic performance, indicating potential and wide application in wastewater

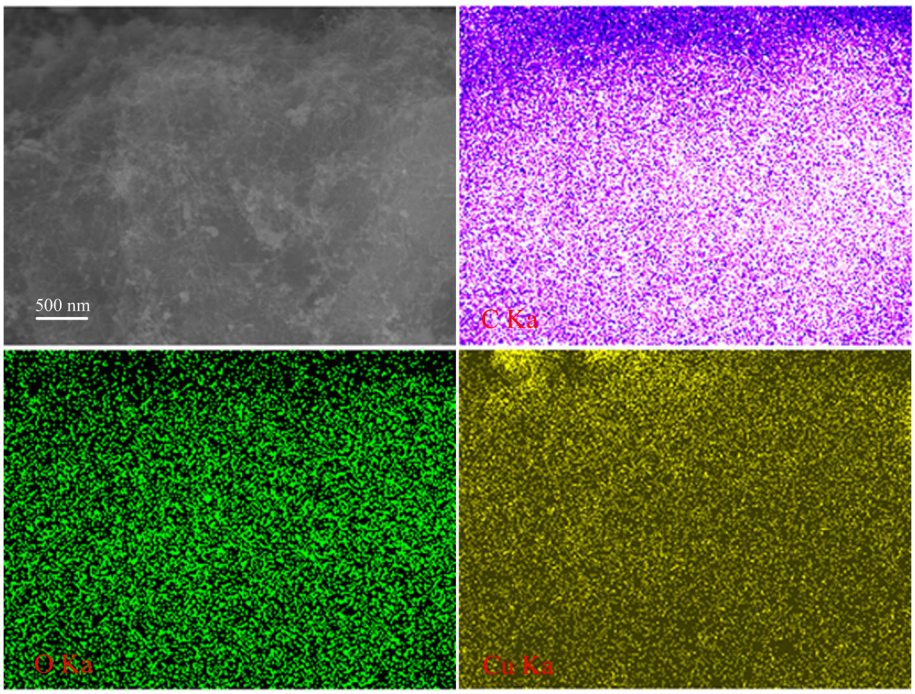

Fig. 2 SEM image of CNT-Cu-30-1 nanocomposite and elemental mappings of C, O, and Cu

treatment and composite materials. The parameters with a reaction temperature of 30 °C with 1 h (CNT-Cu-30-1) could generate the small and uniform Cu_2O nanocrystal in the formed composite material, while increased temperature (CNT-Cu-60-1) and extended preparation time (CNT-Cu-30-6) could produce large agglomerated blocks and obviously decrease the catalytic ability. It was obvious that the size and shape of Cu_2O nanocrystal remarkably impacted on the catalytic activity. Therefore, present work provided potential exploration for the design and preparation of new nanocomposite materials for wide catalytic fields.

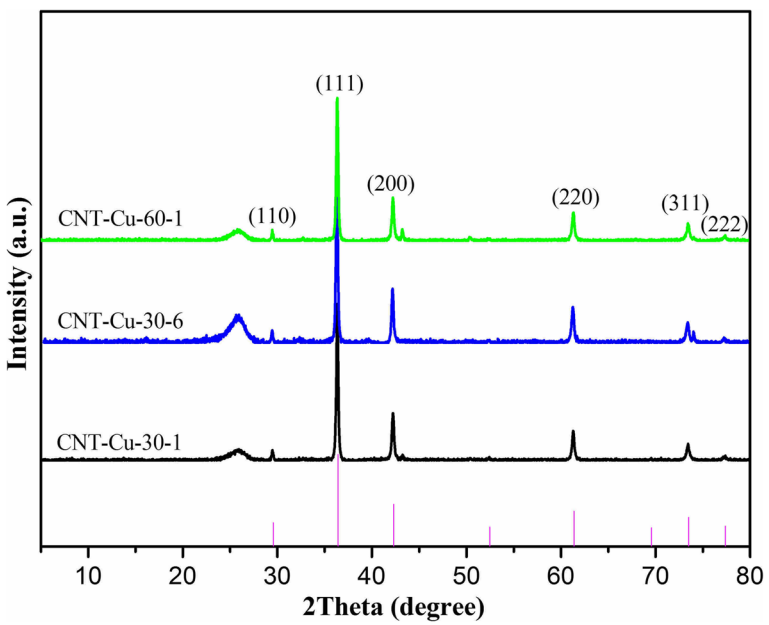

Fig. 3 XRD curves of the synthesized CNT-Cu_2O nanocomposites

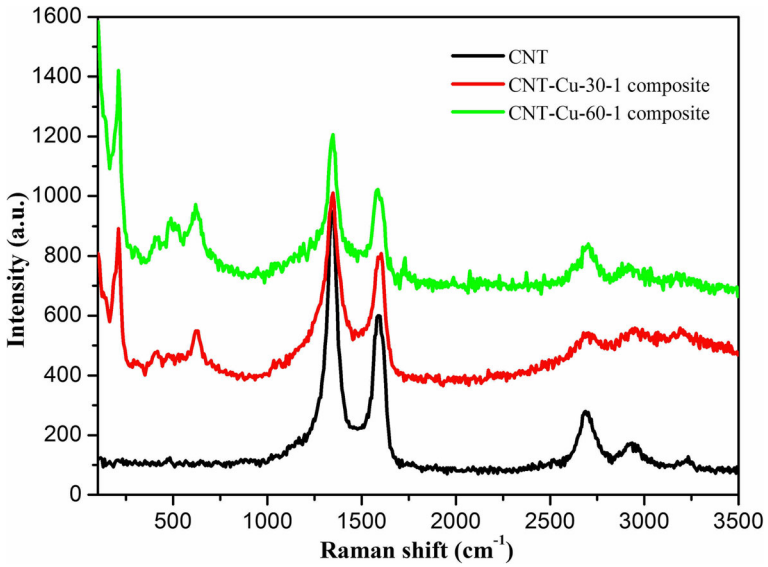

Fig. 4 Raman spectra of the CNT and synthesized CNT-Cu_2O nanocomposites

Conclusions

In summary, we have presented a facile approach to synthesize CNT-Cu_2O nanocomposites by taking advantage of a facile and low-cost method. Through in-depth analysis, the optimized synthesis condition for present CNT-Cu_2O composite was at 30 °C for 1 h, which demonstrated Cu_2O particles with a size of 30–50 nm and uniformly distributed on the surface of CNT. The optimized catalyst product was used for reducing 4-NP reaction to completely form 4-AP just within 35 s. Interestingly, the catalytic ability retained 92% after 8 cycles, which showed the well catalytic stability and potential

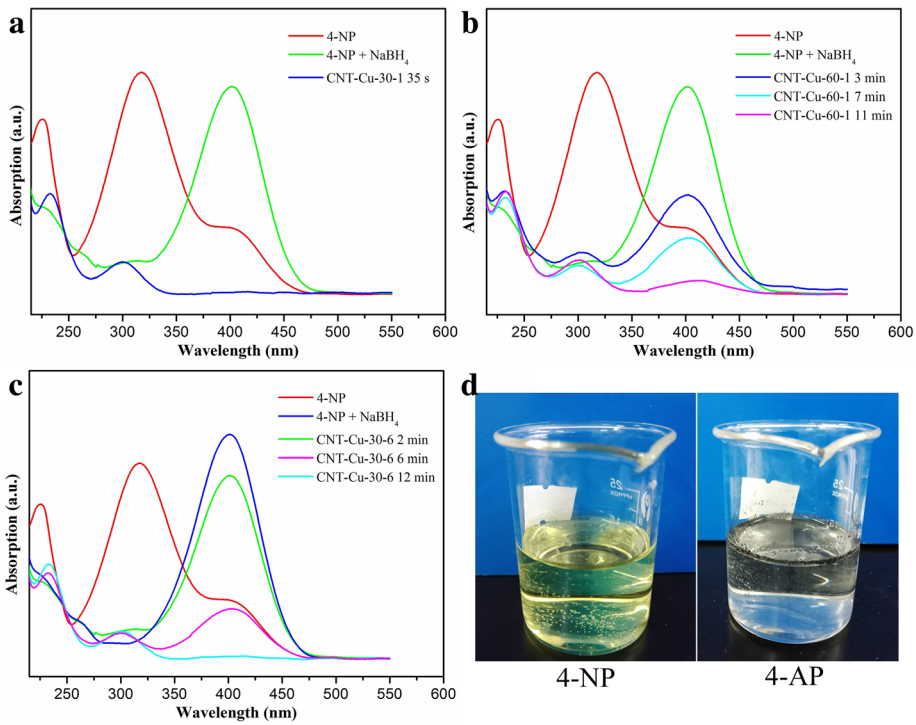

Fig. 5 Catalytic reduction of 4-NP via present synthesized CNT-Cu_2O nanocomposites. **a** CNT-Cu-30-1. **b** CNT-Cu-60-1. **c** CNT-Cu-30-6. **d** The photos of 4-NP solution before and after the catalytic process

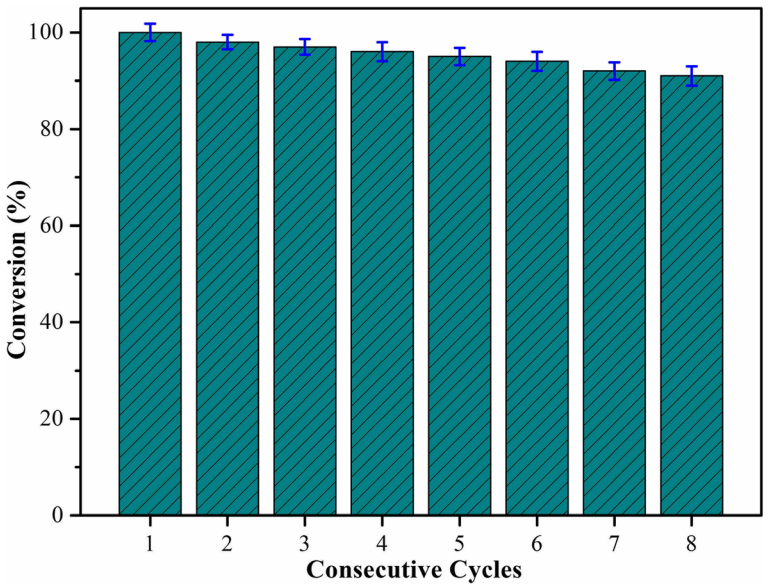

Fig. 6 Reusability test of CNT-Cu-30-1 nanocomposite as a catalyst for the reduction of 4-nitrophenol with $NaBH_4$

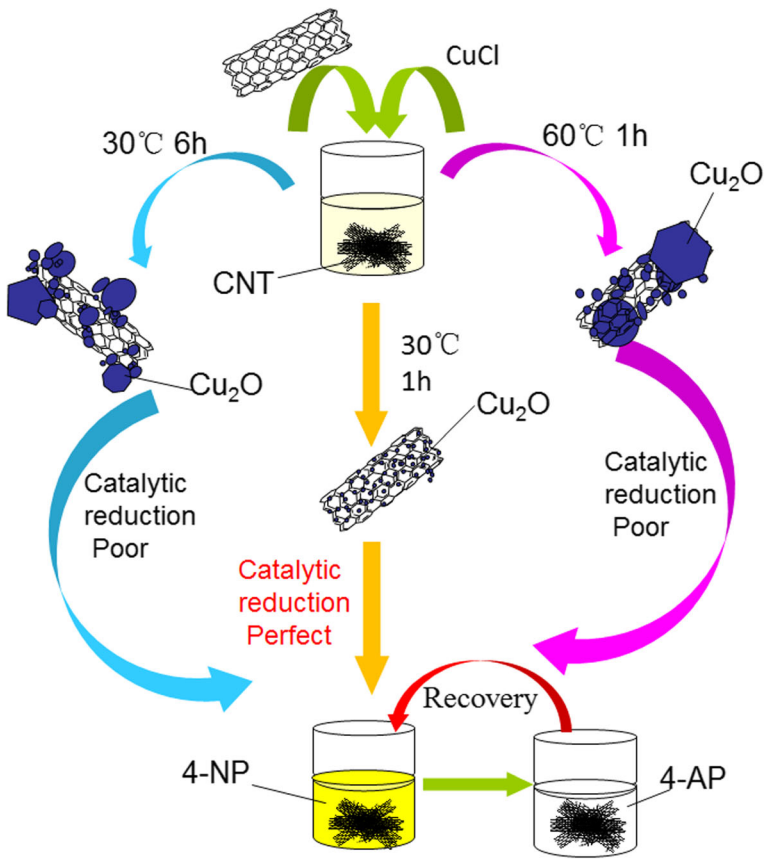

Fig. 7 Schematic illustration of the fabrication and catalytic reduction of the synthesized CNT-Cu_2O nanocomposites

application. The presence of CNT not only provided the function of template substrate, but also improved its mechanical properties and reusability stability. It is found that the synthesized products showed high performance on catalytic reduction of 4-NP even after eight subsequent repeated cycles. Current studies indicated that present synthesized CNT-Cu_2O composite materials could be wide candidates for catalysts in the field of wastewater treatment and composite materials.

Abbreviations

4-NP: P-nitrophenol; CNT: Carbon nanotube; CNT-Cu-30-1: Composite obtained under 30 °C and 1 h; CNT-Cu-30-6: Composite obtained under 30 °C and 6 h; CNT-Cu-60-1: Composite obtained under 60 °C and 1 h; SEM: Scanning electron microscope; TEM: Transmission electron microscope; XRD: X-ray diffraction

Funding

This work was financially supported by the National Natural Science Foundation of China (Nos. 21872119, 21473153), Support Program for the Top Young Talents of Hebei Province, China Postdoctoral Science Foundation (No. 2015M580214), Research Program of the College Science & Technology of Hebei Province (No. ZD2018091), and Scientific and Technological Research and Development Program of Qinhuangdao City (No. 201701B004).

Availability of Data and Materials

All data generated or analyzed during this study are included in this published article.

Authors' Contributions

YF and JY participated in the analysis and the testing of the composite materials. LZ and JZ carried out the synthesis and characterization of materials. TJ and LZ supervised this work, helped in the analysis and interpretation of data, and, together with QP, worked on the drafting and revisions of the manuscript. JZ conceived of the study and participated in its design and characterization. LZ and JZ participated in the design of the study and provided analysis instruments. All authors read and approved the final manuscript.

Competing Interests

The authors declare that they have no competing interests.

Publisher's Note

Received: 18 October 2018 Accepted: 25 February 2019
Published online: 05 March 2019

References

1. Fu P, Xiao Z, Liu Y, Wang L, Zhang X, Li G (2018) Support-independent surface function for efficient Pd loading in catalytic hydrogenation. ChemistrySelect 3:3351–3361
2. Pan XL, Bao XH (2011) The effects of confinement inside carbon nanotubes on catalysis. Accounts Chem Res 44:553–562
3. Xiang X, Zhang WJ, Yang ZP, Zhang YY, Zhang HJ, Zhang H, Guo HT, Zhang XT, Li QW (2016) Smart and flexible supercapacitor based on porous carbon nanotube film and polyaniline hydrogel. RSC Adv 6:24946–24951
4. Kang XH, Mai ZB, Zou XY, Cai PX, Mo JY (2007) A sensitive nonenzymatic glucose sensor in alkaline media with a copper nanocluster/multiwall carbon nanotube-modified glassy carbon electrode. Anal Biochem 363: 143–150
5. Razali M, Kim JF, Attfield M, Budd PM, Drioli E, Lee YM, Szekely G (2015) Sustainable wastewater treatment and recycling in membrane manufacturing. Green Chem 17:5196–5205
6. Merkoci A, Pumera M, Llopis X, Perez B, Valle M, Alegret S (2005) New materials for electrochemical sensing VI: carbon nanotubes. Trac-Trend Anal Chem 24:826–838
7. Karimi-Maleh H, Amini F, Akbari A, Shojaei M (2017) Amplified electrochemical sensor employing CuO/SWCNTs and 1-butyl-3-methylimidazolium hexafluorophosphate for selective analysis of sulfisoxazole in the presence of folic acid. J Colloid Interf Sci 495:61–67
8. Bavandpour R, Karimi-Maleh H, Asif M, Gupta VK, Atar N, Abbasghorbani M (2015) Liquid phase determination of adrenaline uses a voltammetric sensor employing $CuFe_2O_4$ nanoparticles and room temperature ionic liquids. J Mol Liq 213:369–373
9. Lebaschi S, Hekmati M, Veisi H (2017) Green synthesis of palladium nanoparticles mediated by black tea leaves (Camellia sinensis) extract: catalytic activity in the reduction of 4-nitrophenol and Suzuki-Miyaura coupling reaction under ligand-free conditions. J Colloid Interf Sci 485:223–231
10. Imran M, Yousaf AB, Zhou X, Jang YF, Yuan CZ, Zeb A, Jiang N, Xu AW (2017) Pd/TiO nanocatalyst with strong metal–support interaction for highly efficient durable heterogeneous hydrogenation. J Phys Chem C 121:1162–1170
11. Peng K, Fu LJ, Yang HM (2017) Hierarchical MoS_2 intercalated clay hybrid nanosheets with enhanced catalytic activity. Nano Res 10:570–583
12. He LL, Tong ZF, Wang ZH, Chen M, Huang N, Zhang W (2018) Effects of calcination temperature and heating rate on the photocatalytic properties of ZnO prepared by pyrolysis. J Colloid Interf Sci 509:448–456
13. Zhao PX, Feng XW, Huang DH, Yang GY, Astruc D (2015) Basic concepts and recent advances in nitrophenol reduction by gold- and other transition metal nanoparticles. Coordin Chem Rev 287:114–136
14. Avraham E, Westover AS, Itzhak A, Shani L, Mor V, Girshevitz O, Pint CL, Nessim GD (2018) Patterned growth of carbon nanotube forests using Cu and Cu/Ag thin film reservoirs as growth inhibitors. Carbon 130:273–280
15. Liu K, Yuan C, Zou Q, Xie Z, Yan X (2017) Self-assembled zinc/cystine-based chloroplast mimics capable of photoenzymatic reactions for sustainable fuel synthesis. Angew Chem Int Ed 56:7876–7880
16. Lan TX, An R, Liu Z, Li KJ, Xiang J, Liu GY (2018) Facile fabrication of a biomass-based film with interwoven fibrous network structure as heterogeneous catalysis platform. J Colloid Interf Sci 532:331–342
17. Sun YG, Xia YN (2002) Shape-controlled synthesis of gold and silver nanoparticles. J Cheminformatics 298:2176–2179
18. Zou Q, Liu K, Abbas M, Yan X (2015) Peptide-modulated self-assembly of chromophores toward biomimetic light-harvesting nanoarchitectonics. Adv Mater 28:1031–1043
19. Yan X (2017) Bio-inspired photosystem for green energy. Green Energ Environ 2:66
20. Liu K, Xing R, Li Y, Zou Q, Möhwald H, Yan X (2016) Mimicking primitive photobacteria: sustainable hydrogen evolution based on peptide-porphyrin co-assemblies with a self-mineralized reaction center. Angew Chem Int Ed 128:12691–12695
21. Li H, Cooper-White JJ (2013) Hyperbranched polymer mediated fabrication of water soluble carbon nanotube-metal nanoparticle hybrids. Nanoscale 5: 2915–2920
22. Didaskalou C, Kupai J, Cseri L, Barabas J, Vass E, Holtzl T, Szekely G (2018) Membrane-grafted asymmetric organocatalyst for an integrated synthesis–separation platform. ACS Catal 8:7430–7438
23. Sun Y, Zhang F, Xu L, Yin Z, Song X (2014) Roughness-controlled copper nanowires and Cu nanowires-Ag heterostructures: synthesis and their enhanced catalysis. J Mater Chem A 2:18583–18592
24. Tornoe CW, Christensen C, Meldal M (2002) Peptidotriazoles on solid phase: [1,2,3]-triazoles by regiospecific copper (i)-catalyzed 1,3-dipolar cycloadditions of terminal alkynes to azides. J Org Chem 67:3057–3064
25. Rostovtsev VV, Green LG, Fokin VV, Sharpless KB (2002) A stepwise huisgen cycloaddition process: copper (I)-catalyzed regioselective "ligation" of azides and terminal alkynes. J Cheminformatics 41:2596–2599
26. Tiwari VK, Mishra BB, Mishra KB, Mishra N, Singh AS, Chen X (2016) Cu-catalyzed click reaction in carbohydrate chemistry. Chem Rev 116: 3086–3240
27. Meng XG, Zuo GF, Zong PX, Pang H, Ren J, Zeng XF, Liu SS, Shen Y, Zhou W, Ye JH (2018) A rapidly room-temperature-synthesized Cd/ZnS:Cu nanocrystal photocatalyst for highly efficient solar-light-powered CO_2 reduction. Appl Catal B Environ 237:68–73
28. Mccann SD, Stahl SS (2015) Copper-catalyzed aerobic oxidations of organic molecules: pathways for two-electron oxidation with a four-electron oxidant and a one-electron redox-active catalyst. J Cheminformatics 46:1756–1766

29. Gholami Z, Luo GH (2018) Low-temperature selective catalytic reduction of NO by CO in the presence of O_2 over Cu:Ce catalysts supported by multi-walled carbon nanotubes. Ind Eng Chem Res 57:8871–8883
30. Chung M, Nguyen TL, Tran TQN, Yoon HH, Kim IT, Kim MI (2017) Ultrarapid sonochemical synthesis of enzyme-incorporated copper nanoflowers and their application to mediatorless glucose biofuel cell. Appl Surf Sci 429:203–209
31. Hayakawa K, Yoshimura T, Esumi K (2003) Preparation of gold–dendrimer nanocomposites by laser irradiation and their catalytic reduction of 4-nitrophenol. Langmuir 19:5517–5521
32. Esumi K, Hayakawa K, Yoshimura T (2003) Morphological change of gold-dendrimer nanocomposites by laser irradiation. J Colloid Interf Sci 268:501–506
33. Esumi K, Miyamoto K, Yoshimura T (2002) Comparison of PAMAM-au and PPI-Au nanocomposites and their catalytic activity for reduction of 4-nitrophenol. J Colloid Interf Sci 254:402–405
34. Leggiero AP, Trettner KJ, Ursino HL, McIntyre DJ, Schauer M, Zeira E, Landi BJ (2019) High conductivity copper-carbon nanotube hybrids via site-specific chemical vapor deposition. ACS Appl Nano Mater. 2:118–126
35. Cho S, Kikuchi K, Lee E, Choi M, Jo I, Lee S-B, Kawasaki A (2017) Chromium carbide/carbon nanotube hybrid structure assisted copper composites with low temperature coefficient of resistance. Sci Rep 7:14943
36. Zhao X, Jiao TF, Xing RR, Huang H, Hu J, Qu Y, Zhou JX, Zhang LX, Peng QM (2017) Preparation of diamond-based AuNP-modified nanocomposites with elevated catalytic performances. RSC Adv 7:49923–49930
37. Luo XN, Ma K, Jiao TF, Xing RR, Zhang LX, Zhou JX, Li BB (2017) Graphene oxide-polymer composite Langmuir films constructed by interfacial thiol-ene photopolymerization. Nanoscale Res Lett 12:99
38. Li K, Jiao T, Xing R, Xing R, Zou G, Zhou J, Zhang L, Peng Q (2018) Fabrication of tunable hierarchical MXene@AuNPs nanocomposites constructed by self-reduction reactions with enhanced catalytic performances. Sci China Mater 61:728–736
39. Wang C, Sun S, Zhang L, Yin J, Jiao T, Zhang L, Xu Y, Zhou J, Peng Q (2019) Facile preparation and catalytic performance characterization of AuNPs-loaded hierarchical electrospun composite fibers by solvent vapor annealing treatment. Colloid Surf A 561:283–291
40. Sun S, Wang C, Han S, Jiao T, Wang R, Yin J, Li Q, Wang Y, Geng L, Yu X, Peng Q (2019) Interfacial nanostructures and acidichromism behaviors in self-assembled terpyridine derivatives Langmuir-Blodgett films. Colloid Surf A 564:1–9
41. Huang X, Jiao T, Liu Q, Zhang L, Zhou J, Li B, Peng Q (2019) Hierarchical electrospun nanofibers treated by solvent vapor annealing as air filtration mat for high-efficiency PM2.5 capture. Sci China Mater 62:423–436
42. Xu Y, Ren B, Wang R, Zhang L, Jiao T, Liu Z (2019) Facile preparation of rod-like MnO nanomixtures via hydrothermal approach and highly efficient removal of methylene blue for wastewater treatment. Nanomaterials 9:10
43. Zhan F, Wang R, Yin J, Han Z, Zhang L, Jiao T, Zhou J, Zhang L, Peng Q (2019) Facile solvothermal preparation of Fe_3O_4–Ag nanocomposite with excellent catalytic performance. RSC Adv 9:878–883
44. Zhou J, Gao F, Jiao T, Xing R, Zhang L, Zhang Q, Peng Q (2018) Selective Cu(II) ion removal from wastewater via surface charged self-assembled polystyrene-Schiff base nanocomposites. Colloid Surf A 545:60–67
45. Chen K, Li J, Zhang L, Xing R, Jiao T, Gao F, Peng Q (2018) Facile synthesis of self-assembled carbon nanotubes/dye composite films for sensitive electrochemical determination of cd(II) ions. Nanotechnology 29:445603
46. Xing R, Liu K, Jiao T, Zhang N, Ma K, Zhang R, Zou Q, Ma G, Yan X (2016) An injectable self-assembling collagen-gold hybrid hydrogel for combinatorial antitumor photothermal/photodynamic therapy. Adv Mater 28:3669–3676
47. Huo S, Duan P, Jiao T, Peng Q, Liu M (2017) Self-assembled luminescent quantum dots to generate full-color and white circularly polarized light. Angew Chem Int Ed 56:12174–12178
48. Chen K, Yan X, Li J, Jiao T, Cai C, Zou G, Wang R, Wang M, Zhang L, Peng Q (2019) Preparation of self-assembled composite films constructed by chemically-modified MXene and dyes with surface-enhanced Raman scattering characterization. Nanomaterials (Basel) 9:(2) https://doi.org/10.3390/nano9020284
49. Wang C, Yin J, Wang R, Jiao T, Huang H, Zhou J, Zhang L, Peng Q (2019) Facile preparation of self-assembled polydopamine-modified electrospun fibers for highly effective removal of organic dyes. Nanomaterials (Basel) 9:(1) https://doi.org/10.3390/nano9010116
50. Chen K, Jiao T, Li J, Han D, Wang R, Tian G, Peng Q (2019) Chiral nanostructured composite films via solvent-tuned self-assembly and their enantioselective performances. Langmuir https://doi.org/10.1021/acs.langmuir.9b00014
51. Huang X, Wang R, Jiao T, Zou G, Zhan F, Yin J, Zhang L, Zhou J, Peng Q (2019) Facile preparation of hierarchical AgNP-loaded MXene/Fe_3O_4/polymer nanocomposites by electrospinning with enhanced catalytic performance for wastewater treatment. ACS Omega 4:1897–1906
52. Guo R, Wang R, Yin J, Jiao T, Huang H, Zhao X, Zhang L, Li Q, Zhou J, Peng Q (2019) Fabrication and highly efficient dye removal characterization of beta-cyclodextrin-based composite polymer fibers by electrospinning. Nanomaterials (Basel) 9:(1) https://doi.org/10.3390/nano9010127